LBNL-59526
LCC-0149
CBP Tech Note-322

Resistive Wall Instability in the NLC Main Damping Rings

A. Wolski
Lawrence Berkeley National Laboratory, Berkeley, California, 94720.

July 1st, 2004

Abstract

We study transverse coupled-bunch instabilities driven by the resistive-wall impedance in the NLC Main Damping Rings. We compare the growth rates of the different modes predicted by a simple theory using a simplified lattice model with the results of a detailed simulation that includes variation of the beta functions and the actual fill structure of the machine. We find that the results of the analytical calculations are in reasonable agreement with the simulations. We include a simple model of a bunch-by-bunch feedback system in the simulation to show that the instabilities can be damped by a feedback system having parameters that are realistic, and possibly conservative. The noise level on the feedback system pick-up must be low, to avoid driving random bunch-to-bunch jitter above the specified limit of 10% of the vertical beam size.

This work was supported by the Director, Office of Science, High Energy Physics, U.S. Department of Energy under Contract No. DE-AC03-76SF00098.

1 Introduction

Coupled-bunch instabilities in electron storage rings can be driven by higher-order modes (HOMs) in the RF cavities, and by resistive-wall wake fields. The RF cavities in the NLC Main Damping Rings (MDRs) are based on the PEP-II designs and the higher-order modes are highly damped; however the narrow chamber aperture means that the resistive-wall wake fields are relatively strong, and dominate over the cavity HOMs in driving beam instabilities.

The short bunch separation (1.4 ns) and high average current (700 mA) in the NLC Main Damping Rings means that coupled-bunch instabilities are to be expected. Generally, coupled-bunch instabilities in high-current storage rings are damped using bunch-by-bunch feedback systems; the ability to prevent the growth of coupled-bunch instabilities depends on the growth rates and on the bandwidth of the instability spectrum. In this note, we aim to characterize these quantities for coupled-bunch instabilities driven by resistive-wall wake fields in the NLC Main Damping Rings. We also consider some appropriate parameters for a feedback system designed to maintain stability in the beam.

Coupled-bunch instabilities are of concern in the damping rings because of the tight tolerances on beam jitter, set by the performance of downstream systems. In the vertical plane, the jitter specification is a maximum of 10% of the vertical beam size; the vertical emittance of the extracted beam is around 5 pm, so the maximum allowable bunch-to-bunch vertical jitter is of the order 0.5 μm. This means that the feedback system will need to have sufficiently low noise, so as not to introduce beam jitter of this level. The unusual mode of operation of the damping rings compared with conventional storage rings may also place particular demands on the feedback system. In a storage ring where the beam is stored for long periods (as in a third generation synchrotron light source), if the feedback system is operating correctly then the amplitudes of the coupled-bunch modes are kept at a very low level, and the feedback system uses very little power. In the NLC damping rings, fresh bunch trains are injected at a rate of 120 Hz; since the bunches in the incoming trains will have large transverse jitter, the feedback system must be capable of responding to the continual demands placed on it.

As a first step to understanding in detail the requirements for the bunch-by-bunch feedback system in the NLC Main Damping Rings, we consider the coupled-bunch instabilities driven by resistive-wall wake fields. We begin by reviewing the standard theory, and applying it to the case of the MDRs. The theory makes a number of simplifying approximations. In particular, variations of the beta functions around the lattice are neglected, and a “uniform fill” (i.e. every RF bucket is filled with the same amount of charge) is assumed. To try and improve the model, we have developed a simulation code that allows tracking of multiple bunches through a lattice with a realistic variation of beta functions, including synchrotron radiation damping and wake fields. Any fill pattern of bunches in the ring can be specified. The simulation also allows a simple model of a feedback system. We describe the simulation code, and present results applied to the NLC Main Damping Rings, using the specified fill pattern.

2 Estimates of Growth Rates from Analytical Formulae

2.1 Theory of Coupled-Bunch Instabilities

Here, we briefly revisit the standard theory of coupled-bunch instabilities, paying careful attention to the approximations that are used to solve the equations of motion, and determine the growth rates of unstable modes. We follow the treatment given by Chao [1].

The equations of motion for the bunches in the accelerator are:

$$\ddot{y}_n(t) + \omega_\beta^2 y_n(t) = -\frac{N r_0 c}{\gamma T_0} \sum_k \sum_{m=0}^{M-1} W_1(-c\tau) y_m(t-\tau) \tag{1}$$

where

$$\tau = \tau(m,n;k) = kT_0 + \frac{m-n}{M} T_0$$

$y_n(t)$ is the transverse displacement of the nth bunch at snapshot time t; ω_β is the betatron frequency; N is the number of particles per bunch; r_0 is the classical radius of the electron; c is the speed of light; γ is the relativistic factor; $W_1(z)$ is the transverse wake function; M is the total number of bunches in the ring. The summation over k represents a sum over many turns of the ring. It is assumed that the ring is uniformly filled, i.e. that bunches with equal charge occur at perfectly regular intervals throughout the ring. Thus, for $k = 0$, τ represents that time interval between bunch m and bunch n passing a given point in the ring. The indexing is such that bunches with larger n are ahead of bunches with smaller n. Causality requires that:

$$W_1(z) = 0 \quad \text{for} \quad z > 0$$

To understand some of the essential properties of the dynamics described by equation (1), let us consider a somewhat simpler system, namely, one in which the equations of motion are given by:

$$\ddot{y}_n(t) = -\sum_{m=0}^{n-1} a_{nm} y_m(t)$$

This is simply a set of coupled harmonic oscillators; the feature that is missing in this system compared to the system in (1) is the time retardation between the position of one oscillator and its effect on another. The eigenstates of this system are determined by the eigenvectors and eigenvalues of the matrix with components a_{nm}. If the μth eigenvector has components $\tilde{y}_n^{(\mu)}$, and the μth eigenvalue is ω_μ^2, then the motion of the nth bunch when the system is in the μth eigenstate is given by:

$$y_n(t) = \tilde{y}_n^{(\mu)} \mathrm{e}^{-\mathrm{i}\omega_\mu t}$$

The meaning of an eigenstate is that if the positions of the oscillators are given by the components of the corresponding eigenvector at some particular time, then the positions of the oscillators are given by the *same* eigenvector at all later times, with an appropriate phase angle. In general, the state of the system will be described by some mixture of eigenstates. However, the amplitudes of the different eigenstates remain constant in time. In general the eigenstates

will *not* be Fourier modes. However, if the coupling is sufficiently weak that the matrix a_{nm} is nearly diagonal, then the eigenstates will be *close* to Fourier modes, i.e. we can write:

$$\tilde{y}_n^{(\mu)} \approx \mathrm{e}^{2\pi i \mu n/M}$$

Now let us return to the real system of interest, namely, that described by equation (1). The fact that the coupling is retarded in time makes no difference to the fundamental property that the system will have a set of eigenstates, corresponding to the eigenvectors and eigenvalues of the coupling matrix. Since the coupling matrix is not exactly diagonal, the eigenmodes will, in general, not be Fourier modes. However, to find a convenient solution to equation (1), we assume that the coupling is weak enough that the eigenmodes can be approximated by Fourier modes. In other words, we make the ansatz that a solution to equation (1) can be written:

$$y_n(t) = \mathrm{e}^{2\pi i \mu n/M} \mathrm{e}^{-i\Omega_\mu t} \tag{2}$$

We proceed to substitute this solution into equation (1); this shall produce for us an expression for the mode frequency Ω_μ in terms of known quantities. The limitation of this procedure is that since (2) is not an exact solution, it does not correctly describe the evolution of the system with time, but only gives an "instantaneous" picture of the dynamics. In physical terms, if we start with the system in a single Fourier mode, then at some later time a number of other Fourier modes will appear to have become mixed in. If the Fourier modes are close to the eigenmodes of the system, then the mixing will be fairly slow; in the case that the Fourier modes happen to be exact eigenmodes, then no mixing will occur.

The result of substituting the ansatz (2) into the equations of motion (1) is [1]:

$$\Omega_\mu - \omega_\beta = -i \frac{MNr_0 c}{2\gamma T_0^2 \omega_\beta} \sum_{p=-\infty}^{\infty} Z_\perp\left[\omega_\beta + (pM + \mu)\omega_0\right] \tag{3}$$

where $Z_\perp(\omega)$ is the transverse impedance (the Fourier transform of the wake function), and ω_0 is the revolution frequency. The real and imaginary parts of the right hand side give us the growth rate and coherent frequency shift of the mode at some instant of time; the solution is not valid over extended periods.

The resistive-wall impedance is given by [2]:

$$Z_\perp(\omega) = C \frac{c}{\omega} \frac{1 - i\,\mathrm{sgn}(\omega)}{\pi b^3 \delta_{skin} \sigma} \tag{4}$$

where C is the machine circumference; b is the radius of the circular beam pipe; σ is the conductivity of the material of the beam pipe, and the skin depth δ_{skin} is given by:

$$\delta_{skin} = \frac{c}{\sqrt{2\pi\sigma|\omega|}}$$

Keeping only the leading term in the summation from (3), we find that an estimate for the growth rate for the mode with the fastest growth rate driven by the resistive-wall impedance is:

$$\frac{1}{\tau^{(\mu)}} \approx -\frac{MNr_0c^2}{b^3\gamma\omega_\beta T_0\sqrt{2\pi\sigma\omega_0}}\frac{\mathrm{sgn}(\Delta_\beta)}{\sqrt{|\Delta_\beta|}} \tag{5}$$

The betatron tune is $\nu_\beta = N_\beta + \Delta_\beta$, where N_β is the nearest integer to ν_β and Δ_β lies between -½ and +½.

2.2 Application to the NLC Main Damping Rings

It is straightforward to use the resistive-wall impedance (4) and the formula (3) for the frequency shift to calculate the growth rates of the different transverse modes in the NLC Main Damping Rings. The lattice is described in reference [3]; the relevant parameters are given in Table 1.

Table 1

Parameters of the NLC Main Damping Rings.

Beam energy	1.98 GeV
Lattice circumference	3.0×10^4 cm
Mean beam pipe radius: $\frac{1}{C}\int_0^C \frac{1}{b^3}ds$	0.734 cm^{-3}
Beam pipe conductivity (aluminum)	3.2×10^{17} s^{-1}
Bunch charge	7.5×10^9
Harmonic number	714
Fill pattern	3×192 bunches
Horizontal tune	21.150
Vertical tune	10.347
Horizontal damping time	3.63 ms
Vertical damping time	4.08 ms

Equation (3) assumes a uniform distribution of bunches around the ring. The NLC Main Damping Rings will be operated with 3 bunch trains; each train consists of 192 bunches with a 1.4 ns bunch separation. The 66 ns gaps between the bunch trains allow for the rise and fall time of the injection/extraction kickers. We can make estimates of the coupled-bunch instability growth rates assuming that the ring is uniformly filled with 714 bunches at the nominal 1.4 ns separation, but using two different approximations for the bunch charge:

1. We assume that the ring is completely filled with bunches with the nominal bunch charge. This should lead to an overestimate of the growth rates.
2. We reduce the bunch charge to give the same average current that will be in the ring in its usual operating mode. This may give some underestimate of the growth rates.

In practice, the second approximation reduces the growth rates by 20% compared to the first approximation, since 80% of the ring will be filled in normal operation. The growth rates using both approximations are shown in Figure 1 (horizontal modes) and Figure 2 (vertical modes).

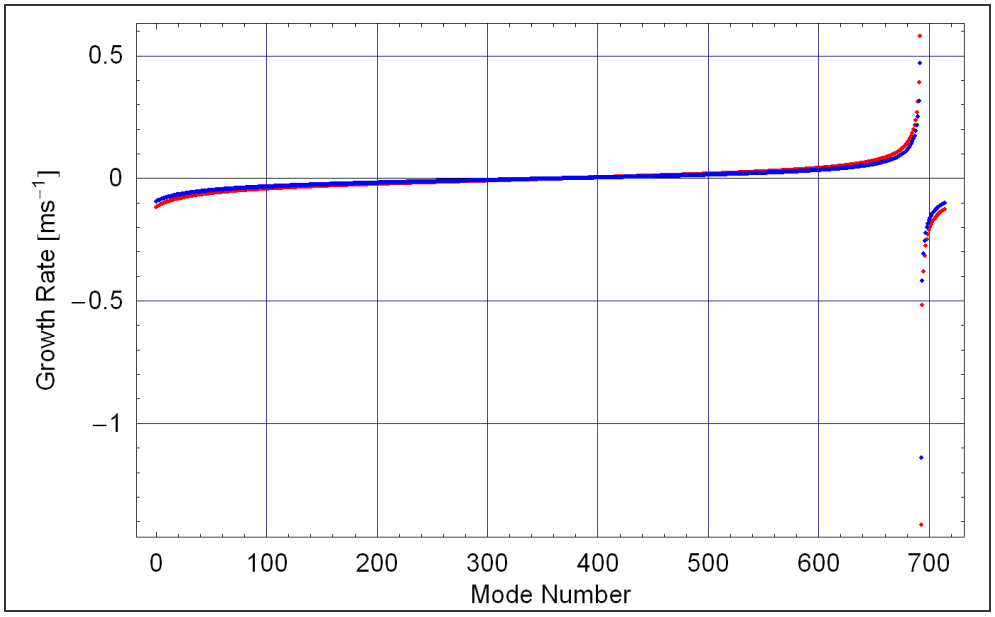

Figure 1

Growth rates of horizontal coupled-bunch modes in the NLC Main Damping Rings. The ring is assumed to be uniformly filled with 714 bunches. Red points show the growth rates assuming the nominal bunch charge. Blue points show the growth rates with the bunch charged reduced to give the same average current as the specified fill, with 3 trains of 192 bunches. Modes with negative growth rates are damped by the resistive-wall impedance.

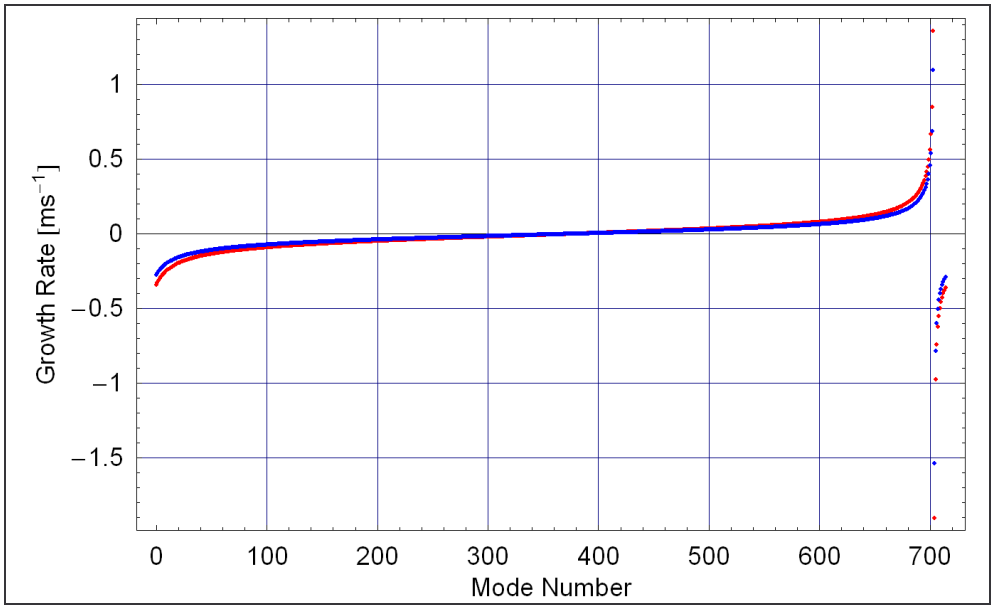

Figure 2

Growth rates of vertical coupled-bunch modes in the NLC Main Damping Rings. The ring is assumed to be uniformly filled with 714 bunches. Red points show the growth rates assuming the nominal bunch charge. Blue points show the growth rates with the bunch charged reduced to give the same average current as the specified fill, with 3 trains of 192 bunches. Modes with negative growth rates are damped by the resistive-wall impedance.

The larger horizontal tune means that the horizontal growth rates are smaller than the vertical; the larger integer part of the tune dominates over the fact that the fractional part of the tune is smaller in the horizontal plane - see equation (5). The fact that the fractional part of the tune is below the half-integer means that in both cases, the most strongly coupled modes are *damped* rather than antidamped.

Some characteristics of the instability are given in Table 2. The highest growth rate expected is in the vertical plane, with a growth rate between 1.1 ms^{-1} and 1.4 ms^{-1}. The bandwidth required of a feedback system to damp the unstable modes is:

$$\Delta f = \frac{\Delta_\beta \omega_0}{2\pi}$$

For the horizontal modes, this is 150 kHz; for the vertical modes, this is 350 kHz. Note that radiation damping should damp the modes with growth rates below the synchrotron radiation damping rate.

Table 2

Growth rates from the resistive-wall impedance in the NLC Main Damping Rings.

	Horizontal modes	Vertical modes
Mode number with fastest growth rate	692	703
Maximum growth rate, specified bunch charge	0.58 ms^{-1}	1.4 ms^{-1}
Maximum growth rate, specified average current	0.47 ms^{-1}	1.1 ms^{-1}

3 Estimates of Growth Rates from Simulation

Instead of using analytical formulae, the equations of motion (1) can be solved by simulation. This allows a more detail model of the system, since a number of approximations needed to find an analytical solution are avoided. We have written a simple tracking code to model coupled-bunch instabilities in storage rings. The particular advantages that this provides over the analytical approach are as follows:

- The correct lattice functions are used, with variation of beta functions around the ring.
- The local beam pipe radius is used, rather than an average around the ring.
- No assumption is made of the form of the solution to the equations of motion. Instead, the exact evolution of the betatron amplitude with time is found for each bunch.
- Any fill pattern may be studied; it is not necessary to assume a uniform fill.
- Effects such as radiation damping and decoherence can be included directly.

The main disadvantage of the simulation is that it can take a long time (up to 24 hours) to produce results. Most of the processing time is used in keeping track of and applying the wake field at each point in the lattice.

3.1 Outline of the Simulation Code

Here we briefly outline the physical models used in the simulation code.

The lattice is modeled as a set of discrete slices. Associated with each slice are: the horizontal and vertical Twiss parameters; the betatron phase advance to the next slice; a wake function; a "history table" recording bunches as they pass through the slice. Specifically, the history table

records the charge, transverse offset (found from the betatron action and phase), and time at which the bunch passes through the slice. For an accurate model, the number of slices should be small compared to the betatron wavelength.

The beam is modeled as a set of individual bunches. Associated with each bunch are: the bunch charge; the position in the lattice; horizontal and vertical betatron actions and phases. Tracking bunches through the lattice without wake fields is straightforward (and very fast). Bunches are initially distributed through the lattice with the required fill pattern. At each time step, the position of each bunch in the lattice is advanced to the next lattice slice, and the betatron phase is advanced accordingly. If the effects of radiation (or decoherence) are to be included, the betatron action is decremented by an appropriate amount.

Tracking with wake fields requires little extra work. The transverse offset of each bunch and its charge is recorded in the history table of each slice as it passes through the slice. In addition, the history table and wake function of each slice is used to calculate the transverse kick on the bunch from the wake field. To limit the size of each history table, an entry is deleted once its contribution to the kick becomes less than a certain fraction of the largest contribution to the kick. The appropriate cut-off can be determined by reducing the cut-off until further reduction leads to no significant change in results. If the cut-off is very small, then a large amount of processor time is required to calculate the wake field kick on each bunch.

The output of the code consists of a table recording the transverse position of each bunch after each turn (or fixed number of turns) around the ring.

3.2 Simulation Results – Uniform Fill

To use the simulation code to model the NLC Main Damping Rings, we divided the lattice into 714 slices, so that the distance between the slices corresponds to the distance between bunches. The distance between the slices is then 0.42 m, which is roughly the same as the minimum beta function, and smaller than the mean beta function of 4 m horizontally, and 7 m vertically.

The wake function at each slice is given (for $z < 0$) by:

$$W_1(z) = \frac{2}{\pi b^3}\sqrt{\frac{c}{\sigma|z|}}\Delta s$$

where Δs is the distance between slices, and b is the local beam-pipe radius at the slice. The cut-off of the wake-field history table is set at 10%, i.e. the record of a bunch passing through the slice is deleted, once the contribution of the wake field from that bunch is less than 10% of the largest contribution of a bunch to the wake field.

To benchmark the code, we considered first a uniform fill, of 714 bunches with a bunch charge of 7.5×10^9 particles. Since the vertical growth rates are much faster than the horizontal, we tracked and applied wake fields only in the vertical plane. Initially, the bunches had a uniform random distribution of betatron phase, and a gaussian distribution of betatron action, with the rms normalized action equal to 50 μm. This represents the specified limit on the injection jitter in the NLC Main Damping Rings. The beam was tracked for 4000 turns (corresponding to 4.0

ms). The results are shown in Figure 3, where the emergence of the unstable modes is clearly apparent. To identify the modes present in the bunch position, we constructed a list with elements:

$$y_n = \sqrt{2J_n}\,e^{i\varphi_n}$$

where J_n is the betatron action and φ_n is the betatron phase of the nth bunch, and performed a Fourier analysis of the list.

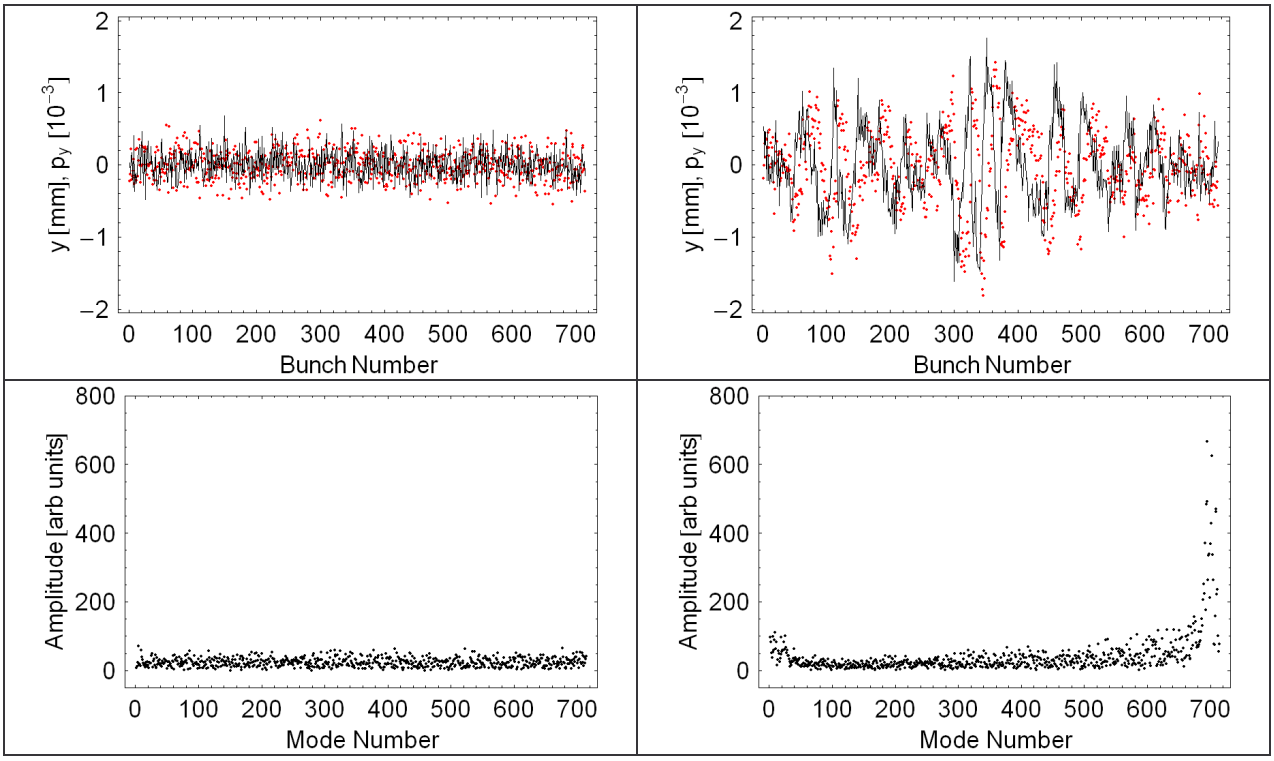

Figure 3

Results of tracking a uniform fill in the NLC MDR, with initial rms normalized vertical action 50 μm. Left plots: initial conditions. Right plots: after 4000 turns (4 ms). The top plots show the vertical co-ordinate (black line) and momentum (red points) of each bunch. The bottom plots show the amplitudes of the Fourier modes in a "snapshot" of the vertical offsets.

To determine the growth rates, we fit an exponential curve to each mode amplitude as a function of time. Some examples are shown in Figure 4. In most cases, the exponential fit to the mode is reasonably good; however, some modes show significant variation. This is expected, since the Fourier modes are not eigenmodes of the system – see the discussion in Section 2.1. Nonetheless, if we compare the growth rates of the different modes obtained in this way with the estimates from equation (3) (the perturbation theory result), the agreement is reasonably good. The comparison is shown in Figure 5 – note that the red line in this figure is the same as the red points in Figure 2. There is significant scatter in the points representing the simulation results; this is because the Fourier modes do not really evolve exponentially with time. There is some evidence of mode mixing in the apparent spread of the peak in the growth-rate curve.

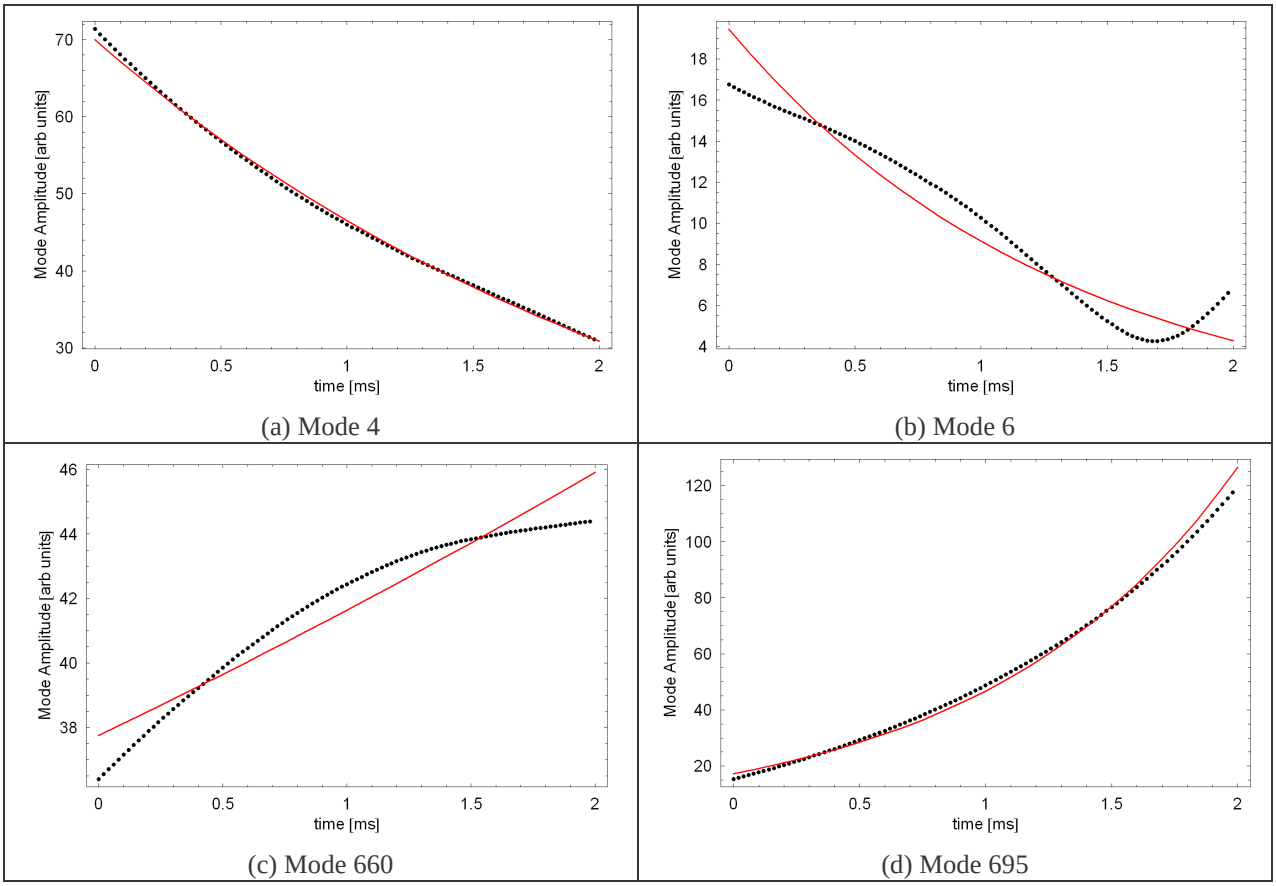

Figure 4

Evolution of selected mode amplitudes with time. Black points show tracking data, red lines show exponential fits.

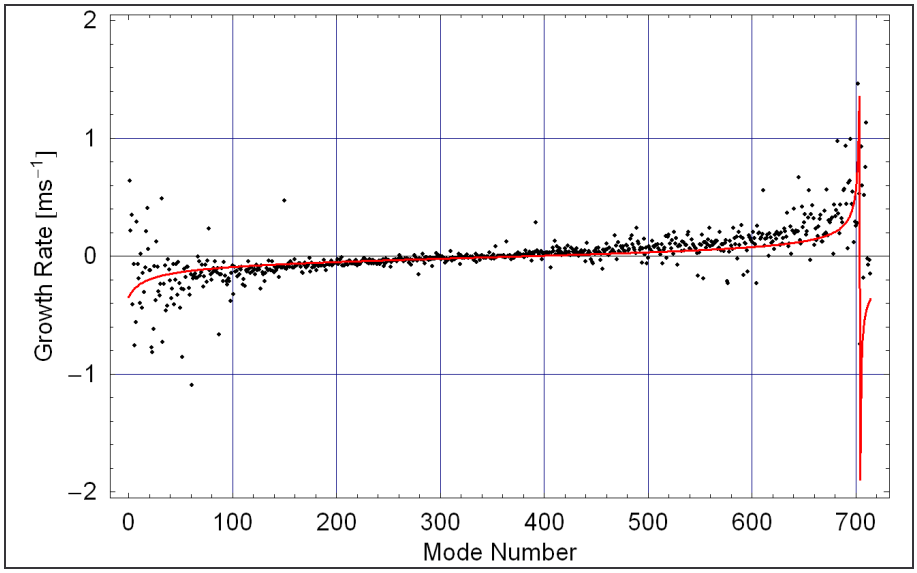

Figure 5

Growth rates of various modes in a uniformly filled ring. Black points: tracking simulation. Red line: analytical estimate. Modes with positive growth rates are unstable.

Importantly, there is good agreement between the maximum growth rates found from the simulation (mode number 702, 1.5 ms^{-1}) and from the analytical estimate (mode number 703, 1.4 ms^{-1}).

3.3 Simulation Results – Fill with 3 Bunch Trains and Radiation Damping

The standard operating mode of the NLC Main Damping Rings will be with 3 trains of 192 bunches, with a gap corresponding to 46 bunches between the bunch trains to allow for the rise and fall of the injection/extraction kicker pulses. We have repeated the simulation reported in Section 3.2 using this fill pattern in place of the uniform fill. We have also included radiation damping. The analysis proceeds as before, except that the mode amplitudes are found by a Fourier analysis of a "completed" fill, formed by inserting bunches with zero betatron action in the gaps between the bunch trains. Thus, the total number of modes present is 714, as in the case of the uniform fill.

The bunch offsets and Fourier mode amplitudes at the start of the simulation and after 4000 turns are shown in Figure 6. As expected, there are some modes that are still unstable. The growth rates are compared with the analytical estimate in Figure 7. The blue line in Figure 7 showing the analytical estimate is the same as the blue points in Figure 2, with the synchrotron radiation damping rate subtracted.

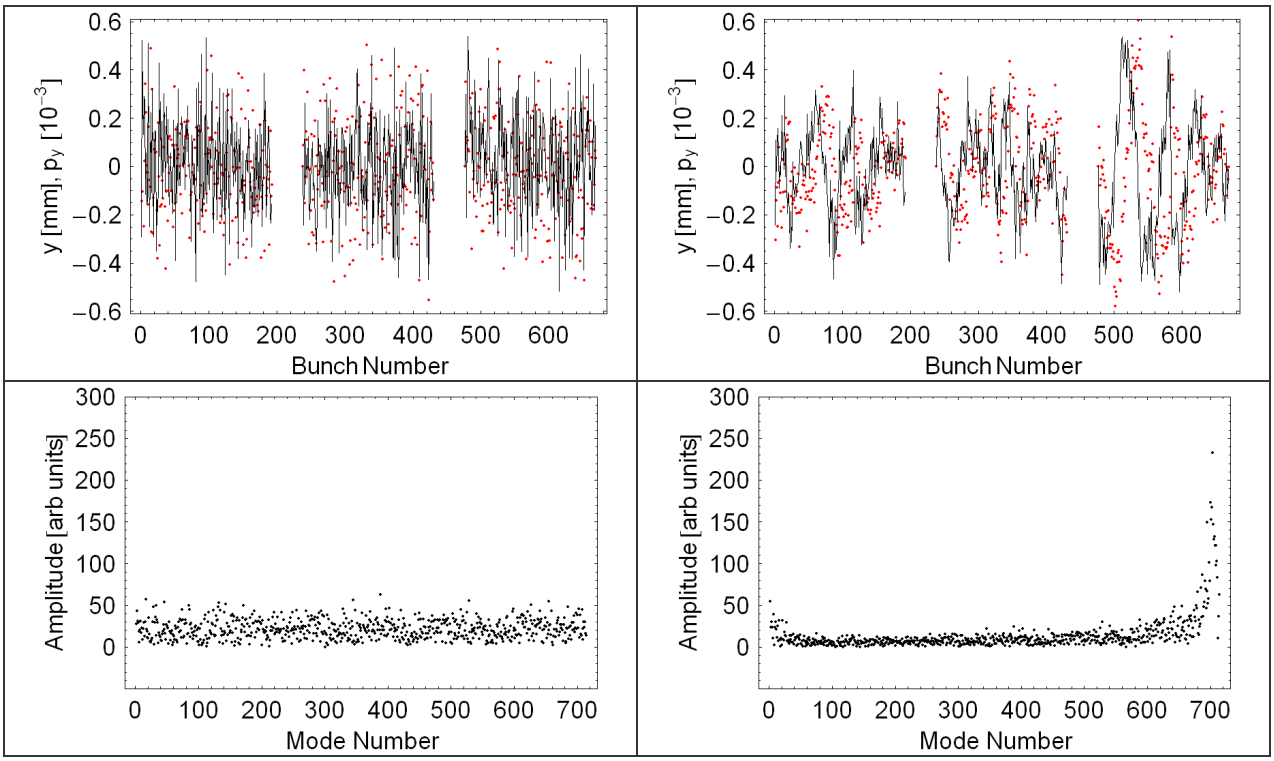

Figure 6

Results of tracking a fill with 3 trains of 192 bunches in the NLC MDR, with radiation damping. The initial rms normalized vertical action is 50 μm. Left plots: initial conditions. Right plots: after 4000 turns (4 ms). The top plots show the vertical co-ordinate (black line) and momentum (red points) of each bunch. The bottom plots show the amplitudes of the Fourier modes in a "snapshot" of the vertical offsets. Note the different scales compared to Figure 3.

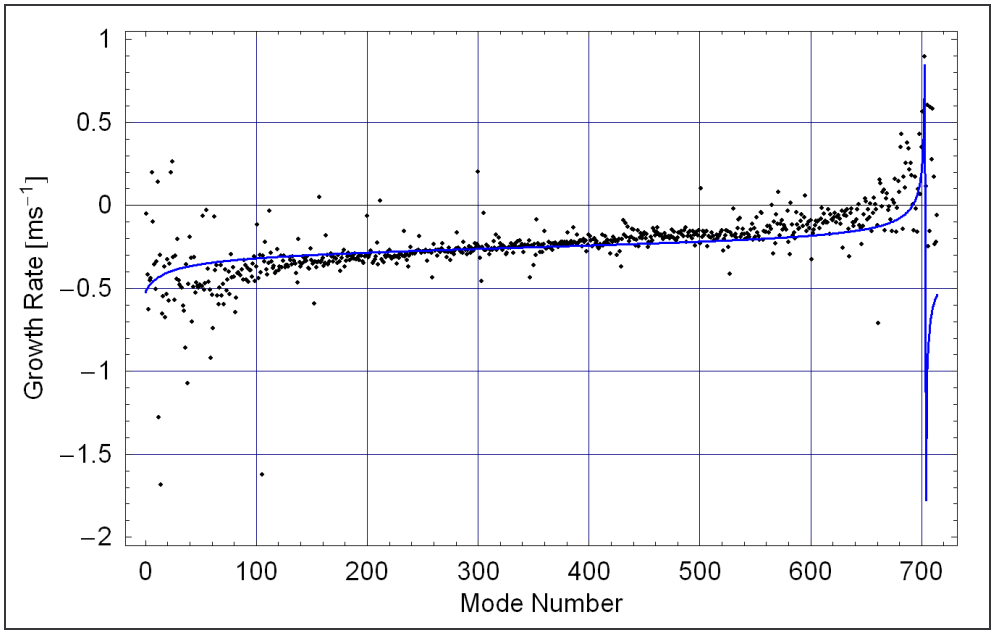

Figure 7

Growth rates of various modes in a ring filled with 3 trains of 192 bunches, including radiation damping. Black points: tracking simulation. Blue line: analytical estimate. Modes with positive growth rates are unstable.

Again, there is good agreement between the maximum growth rates found from the simulation (mode number 703, 0.99 ms^{-1}) and from the analytical estimate (mode number 703, 0.86 ms^{-1}).

4 Bunch-by-Bunch Feedback System

Under normal operating conditions, we expect to see coupled-bunch instabilities in the NLC Main Damping Rings, and a bunch-by-bunch feedback system will therefore be needed to suppress these instabilities. In this section, we consider the required performance of such a feedback system, and present results from simulations of the resistive wall instability, that include a simple model of a feedback system.

Bunch-by-bunch feedback systems can operate in a number of different ways. Here we assume a simple and fairly general model, with a pick-up and a kicker separated by a betatron phase advance of an odd-integer multiple of $\pi/2$. The signal generated by the transverse bunch position at the pick-up is amplified and fed to the kicker. Our model will also include random noise on the pick-up signal and saturation of the kicker pulse. We first consider the appropriate parameters for a bunch-by-bunch feedback system in the NLC Main Damping Rings, and then present the results of simulations of damping of transverse resistive-wall instability using a feedback system.

4.1 Feedback System Parameters

Feedback systems for coupled-bunch instabilities are discussed by Rogers [4]. Here, we briefly review the important formulae.

Suppose the pickup is located at position s_1 in the lattice, where the beta function is β_1. A bunch with transverse action J_1 and betatron phase φ at the pickup will have transverse offset:

$$y_1 = y(s_1) = \sqrt{2\beta_1 J_1}\cos(\varphi)$$

Now suppose the kicker is located at s_2, where the beta function is β_2 and the alpha function is α_2. Let $\Delta\varphi_{21}$ be the betatron phase advance from s_1 to s_2. The action is conserved, so the transverse momentum at the kicker will be:

$$p_{y2} = p_y(s_2) = -\sqrt{\frac{2J_1}{\beta_2}}\left[\sin(\varphi + \Delta\varphi_{21}) + \alpha_2\cos(\varphi + \Delta\varphi_{21})\right]$$

In the particular case that $\Delta\varphi_{21} = \pi/2$, the transverse momentum is:

$$p_{y2} = -\sqrt{\frac{2J_1}{\beta_2}}\left[\cos(\varphi) - \alpha_2\sin(\varphi)\right]$$

Now suppose the signal from the pick-up is transmitted to the kicker with gain g, i.e. the bunch receives a momentum kick at s_2 with strength proportional to the bunch offset at s_1:

$$\Delta p_y = g \cdot y_1 \tag{6}$$

This leads to a change in the betatron action. The change in the action can be calculated from:

$$2J_1 = \gamma_1 y_1^2 + 2\alpha_1 y_1 p_{y1} + \beta_1 p_{y1}^2$$
$$2J_2 = \gamma_2 y_2^2 + 2\alpha_2 y_2\left(p_{y2} + \Delta p_y\right) + \beta_2\left(p_{y2} + \Delta p_y\right)^2$$

where the co-ordinate and momentum are evaluated at s_2. After some algebra, we find:

$$J_2 = J_1\left[1 - 2g\sqrt{\beta_1\beta_2}\cos^2(\varphi) + g^2\beta_1\beta_2\cos^2(\varphi)\right]$$

Over many turns, we can average the phase angle:

$$\left\langle\cos^2(\varphi)\right\rangle = \frac{1}{2}$$

and thus we find:

$$J_2 = J_1\left[1 - g\sqrt{\beta_1\beta_2} + \tfrac{1}{2}g^2\beta_1\beta_2\right] \approx J_1 e^{-g\sqrt{\beta_1\beta_2}} \tag{7}$$

We see that on average, the betatron amplitude (the square root of the action) decays exponentially:

$$J(t) = J_0 e^{-g\sqrt{\beta_1\beta_2}t/T_0} \tag{8}$$

where T_0 is the revolution period.

Suppose we have an unstable coupled-bunch mode, with a growth time τ for the betatron amplitude. The action is the square of the amplitude so the action grows exponentially:

$$J(t) = J_0 e^{2t/\tau} \tag{9}$$

For the feedback system to prevent the instability from growing, then from equations (8) and (9) we require:

$$g \geq \frac{2}{\sqrt{\beta_1 \beta_2}} \frac{T_0}{\tau}$$

Finally, we need to relate the gain g to the voltage pulse at the kicker. If the kicker consists of a pair of electrodes of length L and separated by distance d, then the momentum kick given to a bunch passing between the electrodes when the voltage between them is V, is:

$$\Delta p_y = \frac{1}{cB\rho} \frac{LV}{d} = \frac{\tilde{V}}{cB\rho} \tag{10}$$

where $B\rho$ is the beam rigidity, and we define an "effective voltage" $\tilde{V}$ given by:

$$\tilde{V} = \frac{LV}{d}$$

From equations (6) and (10), we have:

$$\frac{\mathrm{d}\tilde{V}}{\mathrm{d}y} = cB\rho \cdot g = \frac{E}{e} g$$

where we have written the rigidity in terms of the beam energy E. This gives us finally the required gain (expressed in terms of the effective voltage at the kicker per unit bunch offset at the pick-up) in terms of the growth time of the instability we are trying to suppress:

$$\frac{\mathrm{d}\tilde{V}}{\mathrm{d}y} \geq \frac{2}{\sqrt{\beta_1 \beta_2}} \frac{E}{e} \frac{T_0}{\tau} \tag{11}$$

From Section 3.3, we expect a maximum growth rate from the resistive-wall impedance of around 1 ms^{-1}. In the simulation, we shall position the pick-up and the kicker at locations with beta functions β_1 = 5.2 m and β_2 = 6.4 m. Using the parameters from Table 1, we then find that we require:

$$\frac{\mathrm{d}\tilde{V}}{\mathrm{d}y} \geq 690 \text{ V/mm}$$

In practice, a bunch-by-bunch feedback system is not able to provide an unlimited voltage at the kicker, but the voltage will saturate at some level. Also, the pick-up does not have unlimited resolution. The limited resolution may be represented in the model by adding some random number to the signal from the pickup; in our model, we use a Gaussian distribution. To prevent continuously shaking the beam, the system is set so that no voltage is applied to the kicker unless the pickup detects a bunch offset above some minimum level.

The simple model for the bunch-by-bunch feedback system we shall use in our simulations is shown in Figure 8. No voltage is applied to the kicker unless the pick-up detects a bunch with

offset $y > y_{min}$. There is then a linear response up to some maximum voltage V_{max}, at which the kicker voltage saturates.

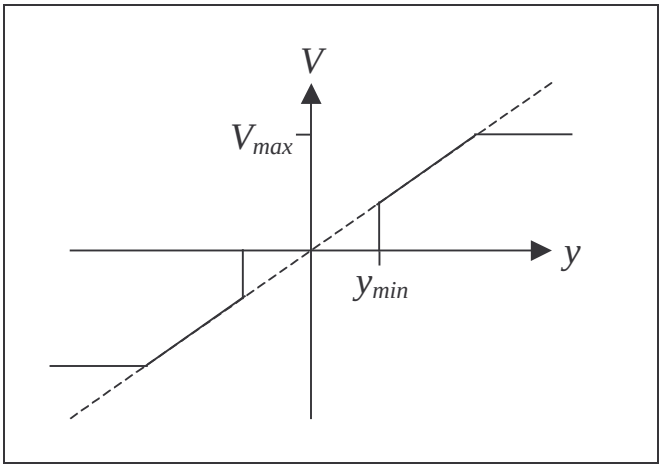

Figure 8

Kicker voltage response to pick-up signal in simple model of a bunch-by-bunch feedback system.

We shall consider two cases for our simulation of the feedback system: the parameters for each case are given in Table 3. The only difference between the cases is the value of the threshold y_{min} and the resolution of the pick-up.

There are a number of other practical issues for the design and operation of feedback systems. For example, closed orbit distortion will give a DC offset to the pick-up signal. There are techniques for dealing with these issues, which we do not consider here: our tracking will be for a perfectly tuned lattice, with no closed orbit distortion.

Table 3

Parameters of bunch-by-bunch feedback system in NLC Main Damping Ring simulations.

	Case I	Case II
Threshold, y_{min}	1.0 μm	0
Pick-up resolution, $\sqrt{\langle \delta y^2 \rangle}$	1.0 μm	5.0 μm
Beta function at pick-up, β_1	5.2 m	5.2 m
Beta function at kicker, β_2	6.4 m	6.4 m
Gain, $\frac{d\tilde{V}}{dy}$	700 V/mm	700 V/mm
Gain, g	3.5×10^{-4} m^{-1}	3.5×10^{-4} m^{-1}
Saturation voltage, V_{max}	100 V	100 V

4.2 Effect of Pickup Signal Noise

The pick-up of the feedback system has a limited resolution. In the simulation, we represent this by adding a random number with a Gaussian distribution to the transverse position of the bunch at the pick-up. It is interesting to consider what the effect of the limited resolution of the pick-up will be on the bunch-to-bunch jitter.

If we replace y_1 in equation (6) by:

$$y_1 \rightarrow y_1 + \delta y$$

then the result in equation (7) is:

$$J_2 \approx J_1 \mathrm{e}^{-g\sqrt{\beta_1\beta_2}} + \tfrac{1}{2}\beta_2 g^2 \delta y^2$$

The noise on the pickup signal gives a term analogous to the quantum excitation that acts with the radiation damping to determine the equilibrium beam size. In the present case, where we are interested in the coherent transverse oscillations of the bunch, we can write the equation of motion for the action, including the effect of the pick-up noise:

$$\frac{\mathrm{d}J}{\mathrm{d}t} = \frac{\beta_2 g^2 \langle \delta y^2 \rangle}{2T_0} - \frac{2}{\tau} J$$

The action reaches an equilibrium:

$$J_{equ} = \frac{\tau}{4T_0} \beta_2 g^2 \langle \delta y^2 \rangle \tag{12}$$

If the feedback system is adjusted to prevent the growth of unstable modes from the resistive-wall impedance, then it is appropriate to set τ equal to the synchrotron radiation damping time.

The specified upper limit on the bunch-to-bunch jitter of the extracted train is that the jitter should be less than 10% of the rms beam size. If ε_y is the rms emittance of the bunch, then the beam size is:

$$\sigma_y = \sqrt{\beta_y \varepsilon_y}$$

Let us write J_y for the coherent transverse action of the bunch, i.e. the action corresponding to the transverse co-ordinate and momentum of the bunch centroid. The maximum transverse co-ordinate is:

$$\langle y \rangle = \sqrt{2\beta_y J_y}$$

The specified upper limit on the bunch-to-bunch jitter can then be written:

$$\frac{\langle y \rangle}{\sigma_y} < 0.1$$

from which it follows:

$$J_y < 0.005\varepsilon_y$$

For a vertical emittance of 5 pm, the coherent transverse action should be less than 0.025 pm. If we use this value for J_{equ} in equation (12), with the values of other parameters as given in Table 3, then we find the upper limit on the noise in the signal from the pick-up:

$$\sqrt{\langle \delta y^2 \rangle} < 5.5 \ \mu\text{m}$$

A pick-up resolution of 5 µm is within the capabilities of modern technology.

4.3 Simulations of Resistive Wall Instability with Feedback System

To approximate the conditions under which the damping ring will operate, we simulate a fill with three bunch trains at different stages of damping. The specified upper limit on the bunch-to-bunch jitter of the injected train corresponds to a mean action of 13 nm (50 µm normalized). The vertical damping time is 4.08 ms, and the repetition rate of the NLC is 120 Hz. We start the simulation with one bunch train just injected, and other bunch trains that have bunch-to-bunch jitter corresponding to storage for 1 and 2 machine cycles, with the effects of radiation damping only (no resistive wall, filamentation or feedback system effects).

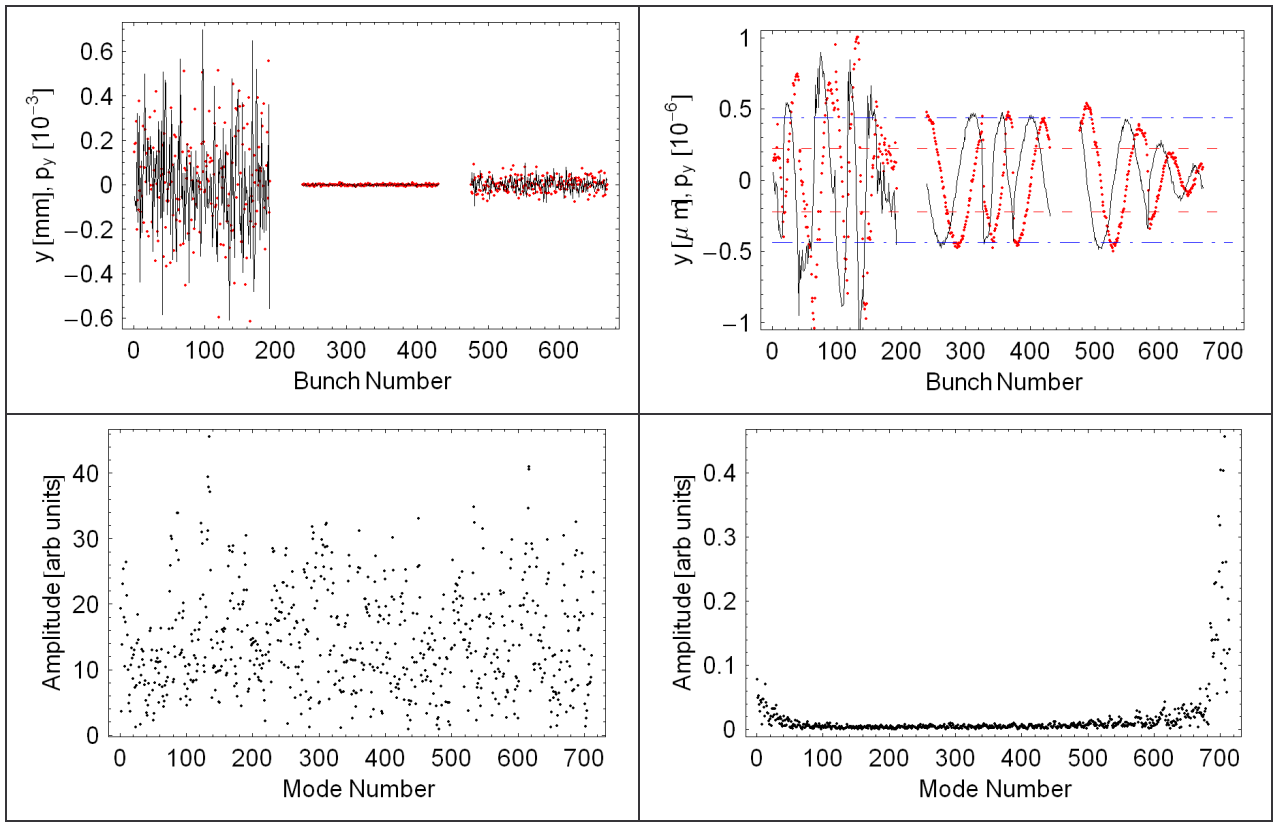

Figure 9

Results of tracking a fill with 3 trains of 192 bunches in the NLC MDR, with different trains at different stages of damping. The feedback system pick-up has a resolution of 1 µm, and a threshold y_{min} of 1 µm (Case I). Bunches with higher bunch number are ahead of bunches with lower bunch number. Left plots: initial conditions. Right plots: after 8333 turns (8.33 ms). The top plots show the vertical co-ordinate (black line) and momentum (red points) of each bunch; the blue dashed-dot lines in the upper left plot shows y_{min} normalized by the beta function; the red dashed line shows 10% of the vertical extracted beam size. The bottom plots show the amplitudes of the Fourier modes in a "snapshot" of the vertical offsets. Note the different scales on the axes of the different plots.

Case I

In this case, the noise in the signal from the pick-up has rms 1 µm, and the threshold value y_{min} is also 1 µm. Figure 9 shows the bunch co-ordinates and spectra at the start of the simulation, and 8333 turns (one machine cycle) later. Note that the co-ordinates are plotted for a "snapshot" of bunches in the ring, with an assumed beta function of 1 m. The beta function at the pick-up is 5.2 m, so the 1 µm value of y_{min} corresponds to 0.44 µm at a beta function of 1 m; this is shown on the plot by the broken horizontal lines. Some of the bunches lie outside this limit, which is possible because of the noise on the pickup signal. The spectrum after one machine cycle is dominated by the modes with the fastest resistive-wall growth rates.

With the parameters given in Table 3, the feedback system should provide additional damping of 1.0 ms^{-1}. A comparison of the growth rates of the different modes found from the simulation with the analytical estimate (including resistive-wall wake fields, radiation damping and feedback system damping) is shown in Figure 10. The feedback system has the expected effect, and all modes are now damped; the theory overestimates the damping slightly, because we have not included the saturation of the feedback system for bunches with large betatron amplitude. Figure 11 shows the evolution of two selected modes over one machine cycle. Figure 12 shows the maximum action of any bunch in each of the three bunch trains as a function of time.

The vertical action of each bunch after 8.3 ms is shown in Figure 13. There appears to be a "transient" along each bunch train; it is not clear if this is a systematic effect. Clearly, the extracted bunch train in the simulation (the central bunch train in Figure 13) does not meet this requirement; the reason is that modes with amplitude below 1 µm at the pick-up are not damped, and this is more than 10% of the beam size at this point.

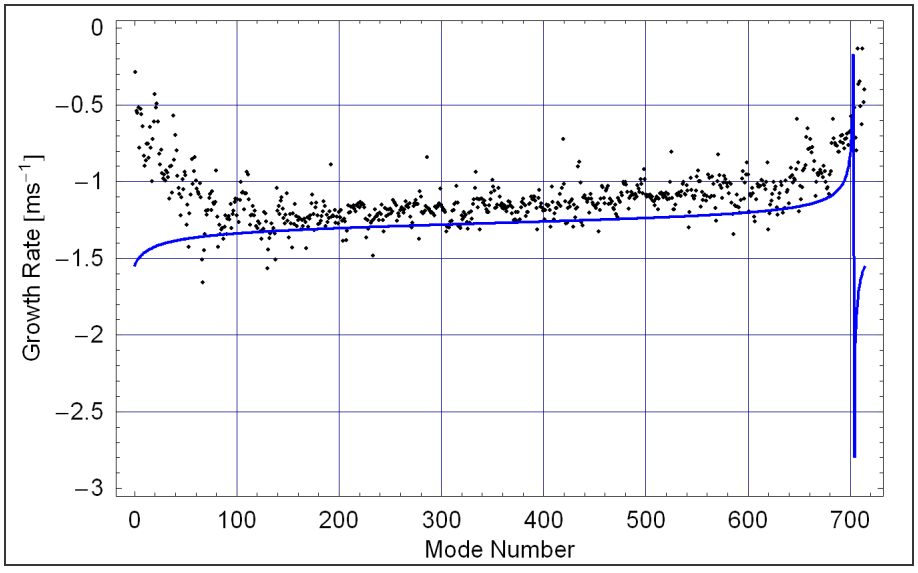

Figure 10

Growth rates of various modes in a ring filled with 3 trains of 192 bunches, including radiation damping and bunch-by-bunch feedback system. Black points: tracking simulation. Blue line: analytical estimate. All modes are damped.

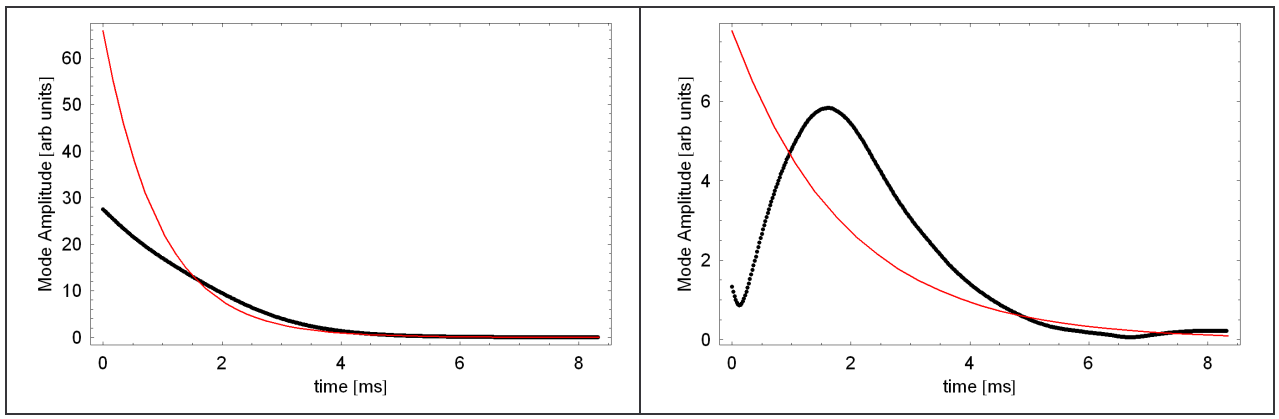

Figure 11

Evolution of two selected mode amplitudes over one machine cycle, for the simulation with 3 trains of 192 bunches, including radiation damping and feedback system. Left: mode 345. Right: mode 702. The black points show the simulation data, the red lines show an exponential fit used to determine the growth/damping rates.

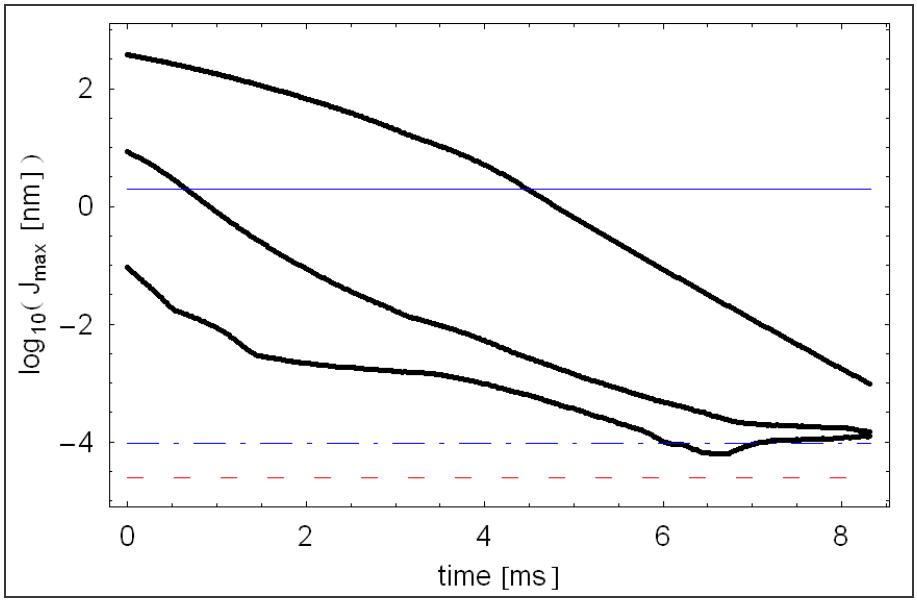

Figure 12

Maximum action of any bunch in each bunch train as a function of time, for the simulation with feedback system Case I. The blue solid line shows the action corresponding to the feedback system saturation level V_{max}. The blue dashed-dot line shows the action corresponding to the feedback system threshold y_{min}. The red dashed line shows the specified bunch-to-bunch jitter limit of 0.025 pm.

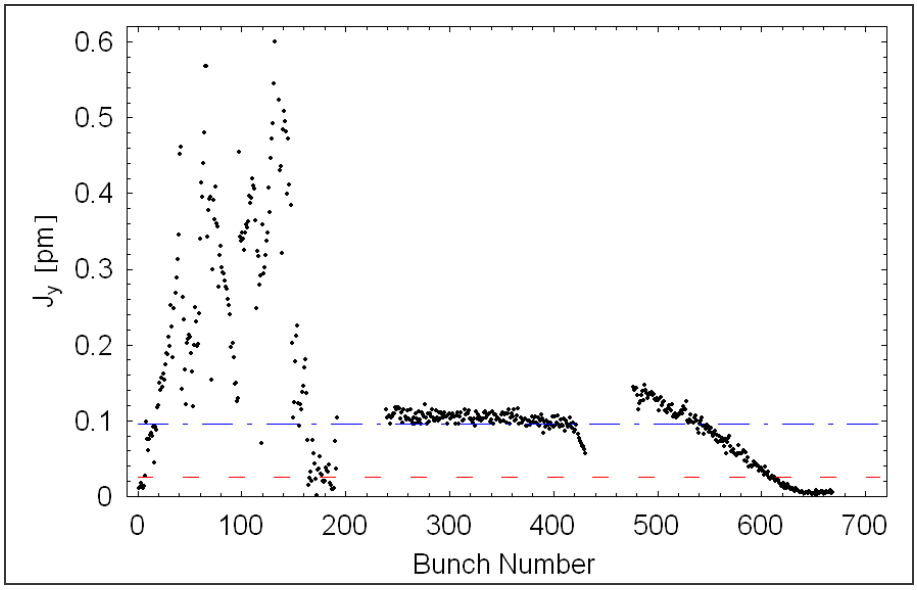

Figure 13

Vertical coherent action of bunches in the damping ring, after 8333 turns in the feedback system simulation, Case I. The central bunch train is the train about to be extracted. The red dashed line shows the specified bunch-to-bunch jitter limit of 0.025 pm. The blue dashed-dot line shows the action corresponding to the feedback system threshold y_{min}.

Case II

In this case, the noise in the signal from the pick-up has rms 5 µm, and the lower threshold value y_{min} is zero; otherwise the simulation is the same as for Case I. In particular, the starting conditions are the same as shown in Figure 9, and we again track for 8333 turns (one machine cycle). The bunch positions at the end of the tracking are shown in Figure 14. It now appears that many more bunches meet the specification on bunch-to-bunch jitter. The vertical actions at the end of the tracking are shown in Figure 16.

Figure 17 shows the distribution of vertical actions in the bunch train about to be extracted. 66% of bunches are within the specified action jitter tolerance of 0.025 pm. The mean action is 0.021 pm. From Figure 14, it is clear that the residual jitter is dominated by the modes that are most strongly driven by the resistive-wall wake fields. The gain of the feedback system has been adjusted so that these modes are damped, but the damping rate is very slow. Increasing the gain of the feedback system would further suppress these modes, but the noise on the pick-up would need to be reduced proportionately, to avoid increasing the random noise on bunch-to-bunch jitter. If we compare Figure 16 with Figure 13, it appears that in Case I (low noise on the pick-up), there is an increasing coherent action from the head to the tail of the bunch train, as would be expected if the transverse oscillations are driven by resistive wall wake fields. In Case II, there is still some systematic increase in the action from the head of the bunch train to the tail, but the random noise is much larger, and of a level consistent with the estimate from equation (12).

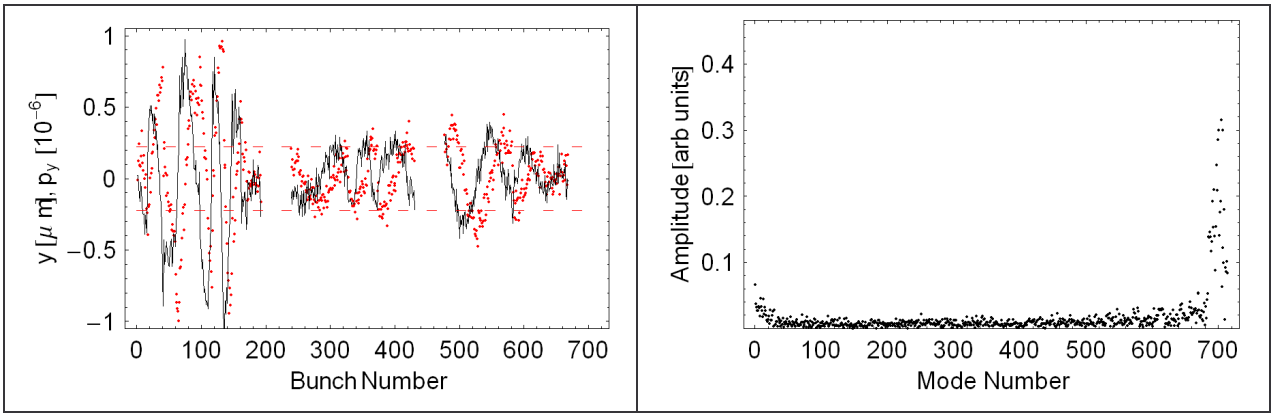

Figure 14

Results of tracking a fill with 3 trains of 192 bunches in the NLC MDR, with different trains at different stages of damping. The feedback system pick-up has a resolution of 5 μm, and a threshold y_{min} of 0 (Case II). Bunches with higher bunch number are ahead of bunches with lower bunch number. The initial conditions are as shown in Figure 9, and the plots here show the bunches after 8333 turns. The left plot shows the vertical co-ordinate (black line) and momentum (red points) of each bunch; the red dashed line shows 10% of the vertical extracted beam size. The right plot shows the amplitudes of the Fourier modes in a "snapshot" of the vertical offsets.

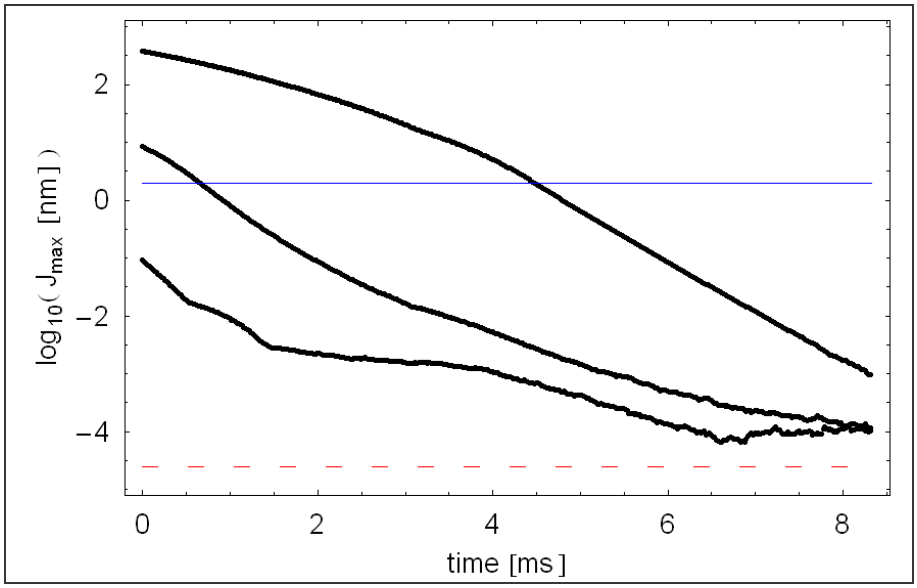

Figure 15

Maximum action of any bunch in each bunch train as a function of time, for the simulation with feedback system Case II. The blue solid line shows the action corresponding to the feedback system saturation level V_{max}. The red dashed line shows the specified bunch-to-bunch jitter limit of 0.025 pm.

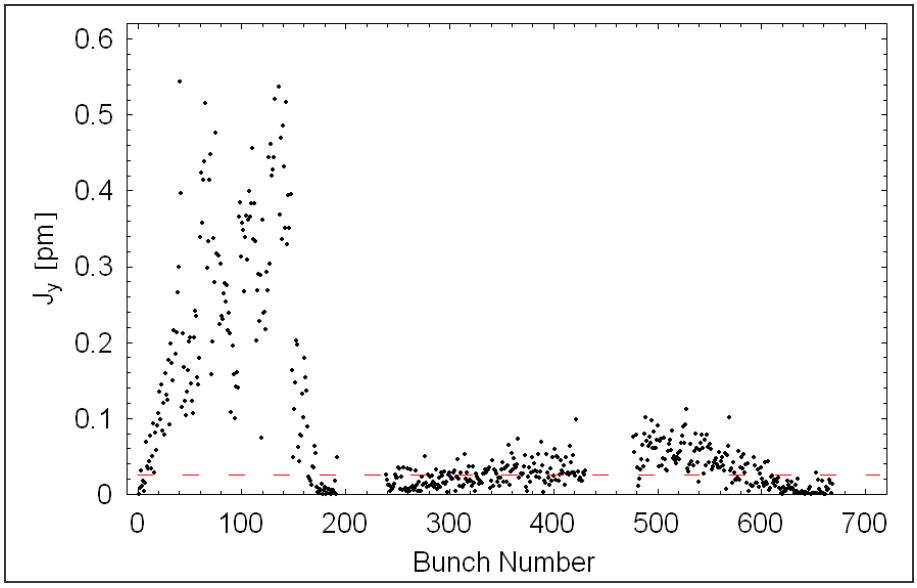

Figure 16

Vertical coherent action of bunches in the damping ring, after 8333 turns in the feedback system simulation, Case II. The central bunch train is the train about to be extracted. The red dashed line shows the specified bunch-to-bunch jitter limit of 0.025 pm.

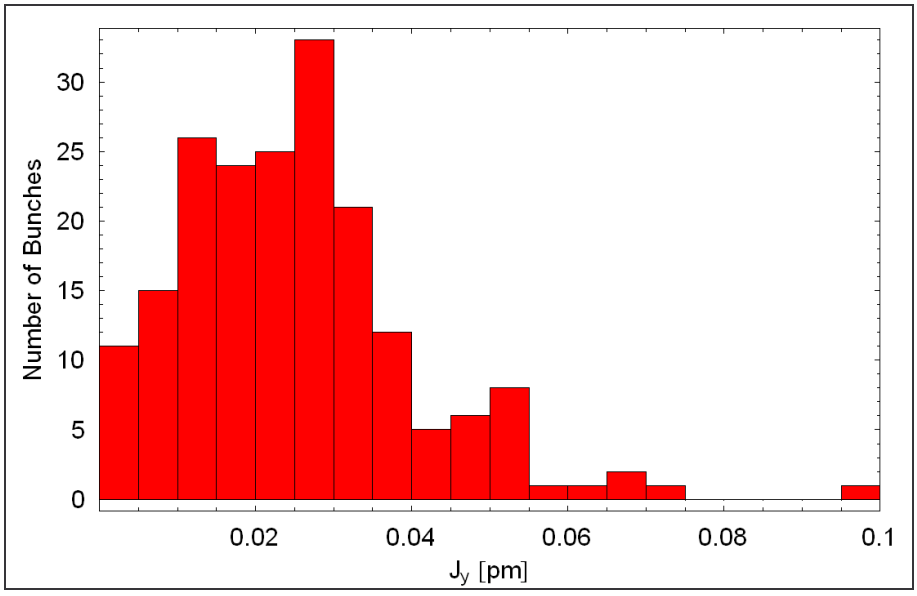

Figure 17

Distribution of vertical coherent action of bunches in the bunch train about to be extracted in the tracking simulation with feedback system, Case II. The specified bunch-to-bunch jitter limit is 0.025 pm; 53% of bunches are within this limit, and the mean action is 0.025 pm.

5 Conclusions and Proposals for Further Work

We have estimated the growth rates of instabilities driven by resistive-wall wake fields in the NLC Main Damping Rings. Analytical estimates, using a number of simplifications, are in good agreement with more detailed simulations. Multi-bunch instabilities will appear in both the horizontal and vertical planes; the vertical growth rates are higher, because the vertical tune is lower than the horizontal tune. The fastest growth rates in the vertical plane are of the order 1 ms^{-1}, and in the horizontal plane of the order 0.5 ms^{-1}.

Bunch-by-bunch feedback systems can be used to suppress the instabilities, and estimates of the parameters suggest that the required performance should be within present capabilities. The noise level on the pick-up must be low (below 5 μm) to avoid driving random bunch-to-bunch jitter above the specified limit of 10% of the vertical beam size.

Further work needs to be done to specify the feedback system more accurately and completely. For example, the value of 100 V that we have used for the saturation voltage (Table 3) is likely to be unnecessarily conservative. The maximum voltage kick depends on the amplifier power and kicker shunt impedance: values for both these quantities vary widely between different systems [5]. However, using typical (though still conservative) values of 150 W for the amplifier power, and 2.5 kW for the kicker shunt impedance, a saturation voltage of 850 V is realistic. Keeping other parameters (gain and beta functions) at the values we assumed in Table 3, the saturation voltage would not be reached until the betatron action were up to 70 times larger than shown by the solid blue lines in Figure 12 and in Figure 15. Although this sounds a large factor, it corresponds to a change in position of the saturation level of less than 2 on the (logarithmic) vertical scale in these plots, and is unlikely to have any real impact on our results. For reducing the bunch-to-bunch jitter on the extracted bunch train, the most significant feedback system parameter is the noise level. Further study is needed to estimate the lowest noise level that can be achieved in a practical system; it is possible that a noise level of around 1 μm may be possible, in which case the system should stay safely below the specified bunch-to-bunch jitter limit.

Although we expect the resistive-wall wake fields to dominate the multi-bunch instabilities, other sources, such as higher-order modes in the RF cavities, should be included. The parameters of the feedback system depend to some extent on the precise implementation, for example through the beta functions at the locations of the pick-up and kicker. Also, some significant effects that could *increase* the damping of the instabilities, such as filamentation, have not been included. However, as filamentation would increase the bunch size, which is highly undesirable, it seems appropriate to design a system in which filamentation is a small effect. All these issues provide topics for further studies.

Acknowledgements

Many thanks to J. Byrd and S. de Santis for useful discussions on resistive-wall instabilities, and for help with constructing a reasonable model for the bunch-to-bunch feedback system used in the simulations presented here.

References

[1] A. Chao, “Physics of Collective Beam Instabilities in High Energy Accelerators”, pp. 203 ff. Wiley, 1993.

[2] A. Chao, ibid., p.71.

[3] M. Woodley and A. Wolski, “The NLC Main Damping Ring Lattice, February 2003”, LCC-0113, February 2003.

[4] J.T. Rogers, “Feedback Systems for Coupled-Bunch Instabilities”, in “Handbook of Accelerator Physics and Engineering”, Ed. A.Chao and M. Tigner, World Scientific 1999.

[5] See, for example: W. Barry, J.M. Byrd et al, “Design of the ALS Transverse Coupled-Bunch Feedback System,” Proceedings PAC 1993. W. Barry, J.M. Byrd et al, “Commissioning of the ALS Transverse Coupled-Bunch Feedback System,” Proceedings PAC 1995. W. Barry, J.M. Byrd et al, “Design of the PEP-II Transverse Coupled-Bunch Feedback System,” Proceedings PAC 1995.